UPPSALA
UNIVERSITET

UPTEC X 19026
Examensarbete 30 hp
Augusti 2019

Development of a method for kinetic characterisation of therapeutic antibodies in solution using the Gyrolab platform

Josef Pelcman

UPPSALA
UNIVERSITET

Teknisk- naturvetenskaplig fakultet
UTH-enheten

Besöksadress:
Ångströmlaboratoriet
Lägerhyddsvägen 1
Hus 4, Plan 0

Postadress:
Box 536
751 21 Uppsala

Telefon:
018 – 471 30 03

Telefax:
018 – 471 30 00

Hemsida:
http://www.teknat.uu.se/student

Abstract

Development of a method for kinetic characterisation of therapeutic antibodies in solution using the Gyrolab platform

Josef Pelcman

Therapeutic antibodies dominate the pharmaceutical market and improve the lives of millions of people annually. One important step when developing new medicines is to kinetically characterise the drug candidates. For antibodies this is difficult since many antibody reactions have extremely slow dissociation rates. By combining a mathematical formula that was recently published with the well-established technology from Gyros Protein Technologies, a new method for full kinetic characterisation was developed and tested in this master thesis. The method provided precise data for five antibodies while also proving to be highly reproducible. By using small sample volumes, unlabelled reagents and having the reaction proceed in solution, this method offers advantages compared to many conventional approaches.

Handledare: Johan Engström
Ämnesgranskare: Magnus Johansson
Examinator: Jan Andersson
ISSN: 1401-2138, UPTEC X19026

Populärvetenskaplig sammanfattning

Antikroppsmediciner har revolutionerat läkemedelsindustrin och hjälper årligen miljoner människor världen över. Nya versioner utvecklas kontinuerlig därmed är även tekniker och metoder som kan bedöma medicinernas verkningsgrad en växande marknad. Rent biologiskt verkar alla mediciner genom att binda till en ligand i kroppen. Därmed är all information om denna bindning av stor vikt då man utvecklar nya mediciner. De kinetiska parametrarna k_{on} och k_{off} är av särskilt intresse då de tillsammans beskriver hur snabbt medicinen binder till proteinet samt hur länge de förblir bundna till varandra.

Men att studera antikroppar kommer med sina svårigheter, de är väldigt dyra så provmängden bör minimeras. Reaktionerna är vanligtvis väldigt långsamma så det är opraktiskt att vänta på att kemisk jämvikt inställer sig, något som vissa metoder idag kräver. Andra tekniker för kinetisk karakterisering kräver att man märker antikroppen eller proteinet den binder till. Denna inmärkning ändrar förstås den kemiska strukturen vilket kan påverka reaktionen. Andra tekniker bygger på att antingen antikroppen eller proteinet är immobiliserat på en yta. Men man kan ifrågasätta hur biologiskt relevanta dessa typer av mätningar är. I kroppen kan båda interaktanterna vara fria i lösning ibland vilket medför att de har andra möjligheter att stöta på varandra och binda.

2018 publicerades en vetenskaplig artikel som beskrev en matematisk modell som kan användas för att beräkna de kinetiska parametrarna innan jämvikt har nåtts. Modellen bygger på att antikropp och protein blandas, sedan mäts koncentrationen av antikroppen vid flera tidpunkter innan jämvikt har nåtts. Syftet med detta examensarbete är att implementera denna modell i företaget Gyros produkter. Gyros producerar mikrofluidiska affinitetskolonner där upp till 112 prover kan koncentrationsbestämmas parallellt. Detta kräver ytterst små provmängder och interaktanterna kan förbli omärkta och reagera fritt i lösning. Med andra ord kringgår denna nya metod många av de begränsningar som dagens tekniker har.

Under projektets gång utvecklades och testades olika sätt att utföra dessa typer av mätningar med Gyros produkter. I slutändan användes den nya metoden för att kinetiskt karakterisera ett mindre antikroppsbibliotek. Metoden har givetvis sina begränsningar, men i diskussionsdelen av denna rapport beskrivs hur man kringgår dessa.

Table of Contents

List of abbreviations 1

Mathematical notations 1

1 Introduction and background 3

1.1 What is an antibody? 3

1.2 Affinity and kinetics 4

1.3 Gyros Protein Technologies 8

1.4 Column profiles 10

1.5 Scope and goals 11

1.6 Motivation 11

2 Material and methods 11

2.1 Materials and consumables 12

2.1.1 Consumables 12

2.1.2 Bioreagents 13

2.1.3 Buffers 13

2.2 Initial experiments with the Bioaffy 1000 13

2.2.1 Detection limit 13

2.2.2 Comparing capture reagent concentrations 14

2.2.3 Determining the kinetic parameters of Humira and TNF-α 14

2.3 Mixing CD 96 14

2.3.1 Reducing the background 16

2.3.2 Wash reagent test 16

2.3.3 Incubation test 16

2.3.4 Comparing the Mix CD with the Bioaffy 1000 17

2.4 Anti-Avastin clones 18

2.4.1 Determining the limit of detection 18

2.4.2 Individual runs 19

2.4.3 Reproducibility test 19

2.4.4 Determining the affinity with the conventional method 19

3 Results 19

3.1 Initial experiments with the Bioaffy 1000 19

3.2 Mixing CD 96 20

3.2.1 Reducing the background 20

3.2.2 Wash reagent test 20

3.2.3 Incubation test 21

3.2.4 Comparing the Mix CD 96 with the Bioaffy 1000 21

3.3 All clones ... 22
3.3.1 Determining the limit of detection ... 22
3.3.2 Individual runs ... 22
3.3.3 Reproducibility test ... 25
4 Discussion ... 26
4.1 Experimental method for pre-equilibrium kinetic characterization using Gyrolab ... 26
4.2 Limitations and how to circumnavigate them ... 26
4.2.1 Reactions with slow dissociation ... 26
4.2.2 Fast reactions ... 27
4.2.3 Biology is complex ... 27
4.2.4 The Bioaffy 96 Mix ... 28
4.3 Column profile analysis ... 29
4.4 Conclusions ... 30
5 Acknowledgements ... 31
6 Bibliography ... 32

List of abbreviations

BSA	Bovine serum albumin
CD	Compact Disc
CV	Coefficient of variation
ELISA	Enzyme-linked immunosorbent assay
Ig	Immunoglobulin
kDa	Kilodalton
K_D	Dissociation constant (M)
k_{on}	Association rate constant ($M^{-1}s^{-1}$)
k_{off}	Dissociation rate constant (s^{-1})
mAb	Monoclonal antibody
S/N	Signal to noise ratio
STD	Standard deviation
M	Molar (mole / L)
PBS	Phosphate buffered saline
PBST	Phosphate buffered saline Tween 20
PCR	Polymerase chain reaction
RU	Response units
TNF-α	Tumour Necrosis Factor-alpha
VEGF	Vascular Endothelial Growth Factor

Mathematical notations

Uppercase letters indicates the variable, whereas lowercase indicates the concentration of said variable. A small letter with a line above indicates the equilibrium concentration. Letters used for variables in this report are a, b, c and t.

X	Molecule X
x	Concentration of molecule X at time t.
$\bar{x}$	Concentration of X at chemical equilibrium.

1 Introduction and background

The field of biotechnology is one of the fastest growing scientific disciplines. It has enabled researcher to learn vast amounts of knowledge about the human body on a cellular level. One field where this is very clear is in medicine; in 2018 seven out of the best selling ten drugs were so called therapeutic antibodies (Urquhart 2019), as showed in figure 1. These are medicines that are made of variants of a large protein, called immunoglobulin G. This has lead to the development of many types of techniques and instruments to facilitate the development and testing of new and improved medicines.

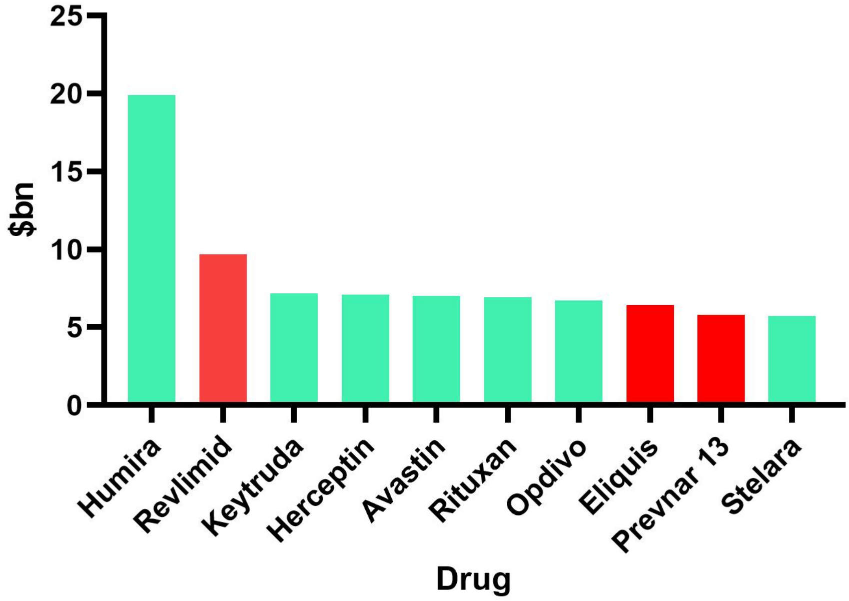

Figure 1: List of the best selling drugs year 2018. The green bars are biological medicines. Figure created in GraphPad Prism 8.0.1. with data from Lisa Urquhart's article (2019).

1.1 What is an antibody?

All forms of life are always under attack from other live forms. We humans are constantly exposed to viruses and bacteria that try to infect our bodies. Thankfully we have evolved to combat this threat and we have specialised cells that mostly keeps us safe. These specialised cells make up our immune system. One cornerstone of the immune system is the production of antibodies, or immunoglobulins *(Ig)*. These are large proteins that are produced and secreted by a special type of cell called B-cells. Antibodies can bind to viruses and bacteria, enabling other immune cells to attack the pathogen. Antibodies can also bind to a toxin and simply render it harmless by blocking the toxin's activity. The binding domain of the antibody is produced in billions of different ways at random, enabling the formation of new antibodies when a new pathogen it present (Alberts *et al.* 2014).

Because antibodies can be produced that effectively binds and neutralizes foreign invaders it was an ideal form of drug for many types of diseases where recognition is of great importance (Chames *et al.* 2009). Antibodies are also very stable proteins, meaning they can last in a persons bloodstream for days. There are five classes of antibodies in humans, IgA, IgD, IgE, IgG and IgM, that all have different functions. But IgG is by far the most abundant in the bloodstream and is the only one used for pharmaceutical purposes.

Two of the drugs showed in figure 1, Humira and Avastin, are used as model systems in this project. Humira binds to the protein Tumour Necrosis Factor Alpha *(TNF-α)* and thereby mitigates its effects in the human body. TNF-α is also involved in the immune system, but is produced in too large quantities in persons who suffer from many autoimmune diseases. By giving these persons Humira, the symptoms of among other arthritis, Crohn’s desease, and psoriasis can be reduced (Burness & Deeks 2012). Avastin on the other hand is used to slow the growth of tumours. It targets a protein called Vascular Endothelial Growth Factor *(VEGF)* that enables the formation of blood vessels at a tumour (Kazazi-Hyseni *et al.* 2010). If the tumour cannot get enough oxygen and nutrient through the blood, it cannot grow larger.

1.2 Affinity and kinetics

When designing new medicines it is of great value to characterize the interaction between the drug molecule and the target protein (Hulme & Trevethick 2010). In this project, I only focus on three constants; the dissociation constant K_D, or what many calls the *“affinity-value”*, the association rate constant k_{on}, and the dissociation rate constant k_{off}. Which are often referred to as the kinetic parameters.

These constants can all be calculated in many different ways, below I will present some simple equations that have helped me get a more intuitive understanding of all these constants.

Say we have a simple bimolecular reaction where molecule A reacts with molecule B to form the complex C:

$$\mathrm{A} + \mathrm{B} \leftrightarrow \mathrm{C}$$

The dissociation constant K_D can be calculated by dividing the equilibrium concentrations:

$$\mathrm{K_D} = \frac{\bar{\mathrm{a}} \times \bar{\mathrm{b}}}{\bar{\mathrm{c}}} \tag{1}$$

So we can think of K_D as a measurement of how much the reaction if offset to the product side. If a reactions K_D value is low, the equilibrium concentrations of the reactants are low. If the K_D value is high, it means that there is less of the product at equilibrium.

The speed that C is formed and again degraded into A and B is given by the dissociation and association rate constants k_{on} and k_{off} and the current concentrations of A, B and C (Pollard 2010).

$$\mathrm{A + B} \underset{\mathrm{k_{off}}}{\overset{\mathrm{k_{on}}}{\rightleftarrows}} \mathrm{C}$$

Knowing this, we can formulate a differential equation describing the flow of C-molecules.

$$\frac{\mathrm{dc}}{\mathrm{dt}} = \mathrm{k_{on}ab - k_{off}c} \tag{2}$$

We can see from equation 2 that at equilibrium (when $\frac{dc}{dt} = 0$) the two terms must be equal, this leads us to a new way of calculating K_D.

$$\mathrm{k_{on}c = k_{off}ab} \Leftrightarrow \frac{\mathrm{k_{off}}}{\mathrm{k_{on}}} = \frac{\mathrm{ab}}{\mathrm{c}} = \mathrm{K_D} \tag{3}$$

There are different ways of solving these equations for K_D, k_{on} and k_{off}, Below is a solution that is applicable when a reaction has reached equilibrium and is used today by Gyros to calculate K_D (Salimi-Moosavi *et al.* 2012).

Since we have a closed system, we can substitute accordingly to reduce the number of variables:

$$\bar{\mathrm{a}} = \mathrm{A_0} - \bar{\mathrm{c}} \tag{4}$$

$$\bar{\mathrm{b}} = \mathrm{B_0} - \bar{\mathrm{c}} \tag{5}$$

Where A_0 and B_0 are the initial concentrations. Inserting this into equation 1 gives:

$$\mathrm{K_D} = \frac{(\mathrm{A_0} - \bar{\mathrm{c}}) \times (\mathrm{B_0} - \bar{\mathrm{c}})}{\bar{\mathrm{c}}} \Leftrightarrow \mathrm{K_D}\bar{\mathrm{c}} = (\mathrm{A_0} - \bar{\mathrm{c}}) \times (\mathrm{B_0} - \bar{\mathrm{c}}) \Leftrightarrow$$

$$\mathrm{K_D}\bar{\mathrm{c}} = \mathrm{A_0B_0} + \bar{\mathrm{c}}^2 - \mathrm{A_0}\bar{\mathrm{c}} - \mathrm{B_0}\bar{\mathrm{c}} \Leftrightarrow \bar{\mathrm{c}}^2 - \bar{\mathrm{c}}(\mathrm{A_0 + B_0 + K_D}) + \mathrm{A_0B_0} = 0$$

This quadratic equation can easily be solved using the quadratic formula (for the positive root):

$$\bar{\mathrm{c}} = \frac{(\mathrm{A_0+B_0+K_D})}{2} + \sqrt{\left(\frac{(\mathrm{A_0+B_0+K_D})}{2}\right)^2 - \mathrm{A_0B_0}} \tag{6}$$

Using non-linear regression this model can be fitted to experimental data and calculate the K_D-value. While this method is quite simple, it can be unpractical to wait for a reaction to reach equilibrium, especially an antibody reaction. Many antibody reactions take hours if not days to reach equilibrium. During this time reagents could degrade or start to react unspecifically

(Vanhove & Vanhove 2018). Also, to only investigate a system at equilibrium says nothing about the kinetic parameters.

In 2018 an article was published by Emilie and Marc Vanhove proposing a solution to these problems. A mathematical formula that solves equation 3 without simplification, giving a function that gives the concentration of the complex C as a function of k_{on}, $k_{off,}$ A_0, B_0 and time. In the article it is solved in the following way (Vanhove & Vanhove 2018):

$$\frac{dc}{dt} = k_{on}ab - k_{off}c$$

Can be integrated to (using equations 4 and 5):

$$\int_0^t \frac{dc}{k_{on}\times(A_0 - c)\times(B_0 - c) - k_{off}c} = \int_0^t dt \qquad (7)$$

and since

$$\frac{1}{k_{on}\times(A_0 - \bar{c})\times(B_0 - \bar{c}) - k_{off}c} = \frac{1}{k_{on}\times c^2 - (k_{on}\times A_0 + k_{on}\times B_0 + k_{off})\times c + k_{on}\times A_0\times B_0}$$

which can be factorized to

$$\frac{1}{k_{on}(c - Y)\times(c - Z)} \qquad (8)$$

where Y and Z, the roots of the quadratic equation, are

$$Y = \frac{(k_{on}\times A_0 + k_{on}\times B_0 + k_{off}) + \sqrt{(k_{on}\times A_0 + k_{on}\times B_0 + k_{off})^2 - 4\times k_{on}^2\times A_0\times B_0}}{2\times k_{on}}$$

$$Z = \frac{(k_{on}\times A_0 + k_{on}\times B_0 + k_{off}) - \sqrt{(k_{on}\times A_0 + k_{on}\times B_0 + k_{off})^2 - 4\times k_{on}^2\times A_0\times B_0}}{2\times k_{on}}$$

we can use partial fraction decomposition to express equation 8 as a sum of rational fractions, which can be integrated:

$$\frac{1}{k_{on}(Z - Y)}\times\left(\frac{1}{c - Z} - \frac{1}{c - Y}\right)$$

and therefore the integral from before can be solved accordingly

$$\int_0^t \frac{dc}{k_{on}\times(A_0-\bar{c})\times(B_0-\bar{c})-k_{off}c} = \frac{1}{k_{on}(Z-Y)}\times\left(\int\frac{dc}{c-Z}-\int\frac{dc}{c-Y}\right) \tag{9}$$

the solution to (9) is

$$\frac{1}{k_{on}\times(Z-Y)}\times\ln\left(\frac{c-Z}{c-Y}\right)$$

replacing Z and Y and rearranging gives

$$-\frac{1}{b}\times\ln\left(\frac{2\times k_{on}\times c-Q+W}{2\times k_{on}\times c-Q-W}\right)$$

where

$$Q = k_{on}(A_0+B_0)+k_{off}$$

$$W = \sqrt{a^2-4\times k_{on}^2\times A_0\times B_0}$$

using this to solve equation 7 gives:

$$-\frac{1}{b}\times\ln\left(\frac{2\times k_{on}\times c-Q+W}{2\times k_{on}\times c-Q-W}\right)+\frac{1}{W}\times\ln\left(\frac{Q-W}{Q+W}\right)=t$$

isolating c gives

$$c=\frac{Q\times(1-c)-b\times(1+c)}{2\times k_{on}\times(1-c)}=$$

$$=\frac{A_0+B_0+{}^{k_{off}}\!/_{k_{on}}}{2}-\sqrt{\left(\frac{A_0+B_0+{}^{k_{off}}\!/_{k_{on}}}{2}\right)^2-A_0\times B_0\times\left(\frac{1+R}{1-R}\right)} \tag{10}$$

where

$$R=\left(\frac{Q-W}{Q+W}\right)\times e^{-W\times t}$$

Equation 10 can be used to model the relationship between the concentrations and the kinetic parameters. But to use it in practice we need to connect it to say, a fluorescent signal P. This is easily done if the signal P is directly proportional to the concentration of one component of the reaction. For the experiments presented in this report, we will always measure the concentration of the molecule A. Thanks to equations 4 and 5 we can write the following expression:

$$P=P_0\times\frac{a}{A_0}=P_0\times\frac{A_0\text{-}c}{A_0}\Leftrightarrow$$

$$P = P_0\times\frac{1}{A_0}\left(A_0-\frac{Q\times(1-R)-W\times(1+R)}{2\times k_{on}\times(1-R)}\right) \tag{11}$$

To use this equation in practice to deduce the kinetic parameters, one needs to analyse several reactions, where the concentration of A is fixed and the concentration of B is varying. These reactions are then stopped at different times and the concentration of free A is measured. This fits perfectly to be implemented into Gyros platform since many samples can be analysed in parallel.

There are other benefits with this method. The molecule A does not need to be labelled with any detection agent, meaning that the reaction is not altered in any way and the reaction itself takes place in solution (Vanhove & Vanhove 2018). Many biosensors work on the principle that one molecule is immobilised to a surface and the other one is flowed above it. However, this is not entirely biologically accurate since it effects the diffusion of the molecules.

1.3 Gyros Protein Technologies

Gyros Protein Technology is a company located in Uppsala. Their main product is a microfluidic device that can measure the concentration of analytes. The microfluidic device, called the Gyrolab Bioaffy, is shaped like a CD, and contains up to 112 affinity columns as seen in figure 2. Just like an ordinary CD the Bioaffy is spun and the resulting centrifugal force drives the flow of fluids. This means that there is no need for pumps. The main advantages of this device are the small sample volume required, and the possibility to analyse over one hundred samples simultaneously (Honda *et al.* 2005, Andersson *et al.* 2007).

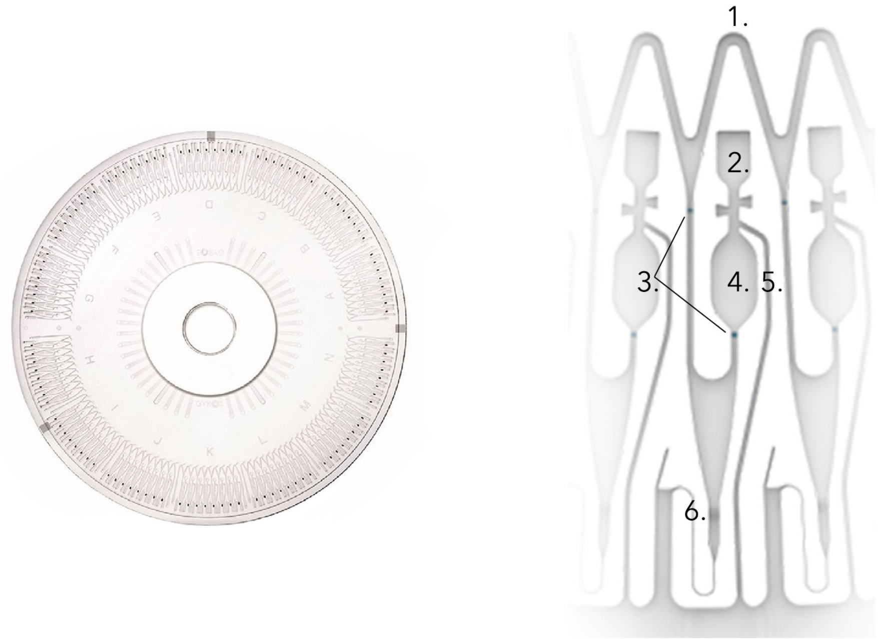

Figure 2: The microfluidic device. The left image shows the entire disc. To the right is a magnification showing three individual affinity columns. 1. The Common Channel, which is used to add solutions that are shared with all samples, such as wash buffers, fluorescent reagents, etc. 2. Inlet for individual sample addition. It is here that the analyte is added. 3. Hydrofobic stops. These hydrophobic barriers enable the precise volume definition to take place entirely on the CD. Fluids are drawn into channels and chambers via capillary forces until the meniscus encounters a hydrofobic stop. When the CD is later spun, the centrifugal force forces the fluid over the stop. 4. Volume definition chamber. The size of this chamber decides the volume of the analyte that is used. 5. Overflow channel. The excess liquid leaves through this channel when the CD is spun, making the sample volume precisely the volume of the definition chamber. 6. Affinity capture column. This ~15 nL sized column contains streptavidin coated beads. This enables the user to customize the experiments by using biotinylated capture agents. Images from Gyros publication material used with permission.

The Bioaffy CD:s would be of no use if not for the instruments that operates them. These instruments, called Gyrolab xPlore and xPand, transfers the reagents from a microtiter plate to the CD, spins the CD in the right sequence and at precise speeds. The instrument also preforms the measurements of the affinity column.

Gyros have made functional prototypes of a wide variety of different microfluidic devices, all based on the CD-principle. It has, among other things, been possible to preform Pyrosequencing (Eckersten *et al.* 2000) and Matrix Assisted Laser Desorption/Ionization Mass Spectrometry (MALDI-MS) pre-treatment (Gustafsson *et al.* 2004). But the application that reached commercial success was a miniaturized immunoassay.

Almost all of the assay formats that are used today, and all that I used in my project, are based on the same steps.

1. First a biotinylated “Capture”-reagent is added to the column. Since the beads are coated with streptavidin the capture reagent will be firmly immobilised to the beads.
2. Secondly the analyte is flowed over the column. The analyte must have some affinity to the biotinylated capture reagent for it to adhere to the column. Often in Gyros applications the capture reagent is an antigen and the analyte is an antibody.

3. Lastly a detection reagent is added. This reagent has a fluorophore linked to it, making it detectable with a spectrophotometer. If the analyte is an antibody, the detect reagent is most often an antibody that has affinity to the analyte. For example, if one examines a therapeutic antibody, it is most likely a human immunoglobulin G. Therefor one chooses an anti-human antibody for the detection reagent.

1.4 Column profiles

The Gyrolab calculated the fluorescence by scanning the column and integrating the pixel intensity of the generated image (Honda *et al.* 2005, Andersson *et al.* 2007). But the software also generated a three dimensional figure by plotting the pixel intensity against the coordinates (See figure 3). This figure, or *column profile*, is mainly used to identify outliers. It has been suggested however that the shape of column profile is dependant on the affinity and kinetics between the solid phase and the liquid phase (Honda *et al.* 2005). This is rather intuitive, the faster the analyte's on-rate is, the more should bind in the very beginning of the column, and the faster the off-rate is the larger the tail-section should be. In fact, analysis of the column profile has been used by researcher to rank the binding strengths of antibodies (Giuliani *et al.* 2018).

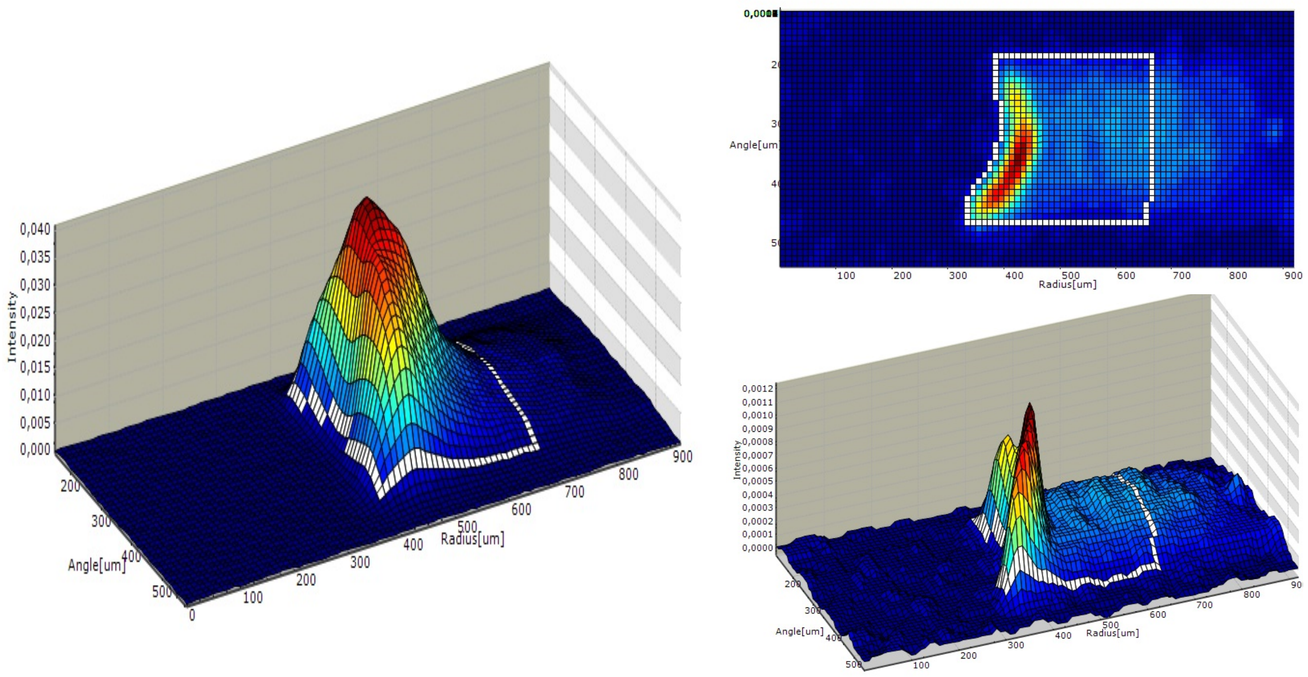

Figure 3: A three dimensional surface plots with the coordinates in the X/Y-plane and the pixel intensity along the Z-axis. To the left side is an ideal profile. On the right side we see two views of poorer data, where it appears that a dust fibre has entered the column. By manually examining the profiles it is easy to identify outliers such as this one. Figures from Gyrolab Evaluator.

1.5 Scope and goals

The project given to me had a well-defined scope, and while the goals were already set, it was entirely up to me to plan and design my own experiments. Below is a list of goals and an outline of the project that was given to me in the beginning of the project by my supervisor.

1. Literature study to get familiar in the area of affinity and kinetic determination including the publication with the suggested pre-equilibrium model.
2. Set up a relevant model system for affinity measurement using Gyros affinity application.
3. Design initial experiments in order to evaluate the results with the pre-equilibrium model.
4. Implementation of the new pre-equilibrium model using suitable software for the analysis.
5. Optimize the experimental set-up in order to determine accurate kinetic and affinity constants especially for high affinity therapeutic antibodies.
6. Compare different bimolecular interactions *(high and low affinity)* and find the limitation of the new methodology.
7. Evaluate the opportunities to use different CD-products including the mixing CD.

1.6 Motivation

Should my project lead to the development of a new tool it would enable Gyros to expand its applications to include kinetic characterization. While this would be desirable for Gyros, it would also benefit society as a whole. Today a few companies dominate the kinetic characterization market. If Gyros can compete with these companies it might lead to drop in prices, making the instruments more accessible for researches around the world. And this approach would potentially mimic the biological environment more closely since the reaction would take place in solution and possibly with the biological matrix still present. Hopefully this would in turn lead to new medicines being developed faster. Having more and better drugs on the market would in turn increase competition, making medicines more available for the people that need them the most.

2 Material and methods

For all of the experiments preformed on the Bioaffy CD:s, an indirect assay was used. This consist of four main steps, first the *Capture reagent* is added. This capture reagent is often a biotinylated form of an antigen. Next the *Analyte* is added, in my experiments this is always an antibody. Lastly the *Detection regent* is added. This is an antibody that is specific to the analyte antibody. The detection antibody has a fluorophore named Alexa 647 linked to it. The resulting complex, which is illustrated in figure 4 below, is then measured using fluorescence. The signal being proportional to the amount of captured analyte.

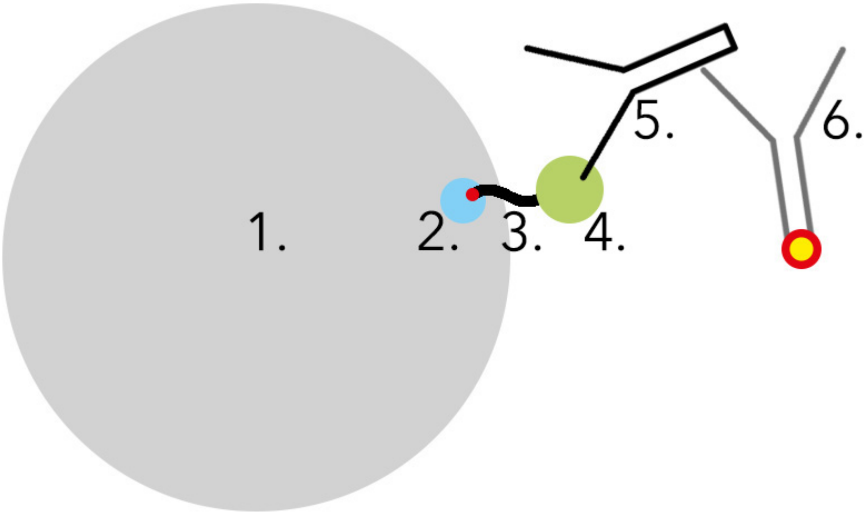

Figure 4: A schematic drawing of how the components are interacting in the column. The large grey bead (1) represents the column matrix, to which streptavidin is bound (2). The capture agent which here is biotinylated TNFα (4) is bound through a linker (3). Humira (5), binds to the TNFα and finally an anti-human antibody binds to the clone. This antibody has a fluorophore attached to it (6), which enables the detection.

2.1 Materials and consumables

2.1.1 Consumables

Product	Supplier
Gyrolab Bioaffy 1000	Gyros Protein Technologies (Uppsala)
Gyrolab Bioaffy 1000HC	Gyros Protein Technologies (Uppsala)
Gyrolab Bioaffy 200	Gyros Protein Technologies (Uppsala)
Gyrolab Mixing CD 96	Gyros Protein Technologies (Uppsala)
Microtiter plate	Gyros Protein Technologies (Uppsala)
Microtiter plate foil	Gyros Protein Technologies (Uppsala)

2.1.2 Bioreagents

Product	Supplier
Humira	Apoteket
Avastin	Roche Biosciences (Palo Alto)
Avastin anti-idiotypes clones	BioGenes (Berlin)
TNFα	ProSpec (Rehovot)
Biotinylated Avastin	*Made in-house*
Biotinylated BSA	Vector Laboratories (Burlingame)
Alexa tagged JDC-10	Southern Biotech (Birmingham)
Alexa tagged anti-mouse lgG	US Biological (Salem)
EZ-Link sulfo NHS-LC-Biotin	Thermo Fischer Scientific (Waltham)

2.1.3 Buffers

Product	Supplier
Rexxip A	Gyros Protein Technologies (Uppsala)
Rexxip F	Gyros Protein Technologies (Uppsala)
PBS	Fisher Bioreagents (Göteborg)
PBST	Fisher Bioreagents (Göteborg)

2.2 Initial experiments with the Bioaffy 1000

The first part of my project was to learn how to use the Gyrolab instrument and then design an assay that would enable a reaction series to be measured at different times. For this sub-project I used a model system consisting of the therapeutic antibody Humira and its target protein TNF-α. As seen in figure 1, Humira is the best selling drug in the world by a huge margin, so using it was thought to be a perfect model system. It is well characterized and there are values for K_D, k_{on} and k_{off} that I could compare my values to.

2.2.1 Detection limit

The first step was to determine the limit of detection of Humira. This was done to later be able to select a suitable concentration of the antibody in future assays.

Humira was diluted from the stock with Rexxip A to 164 nM. From here a dilution series of 15 steps was made down to 0.0250 pM. The Detection antibody was diluted to 12.5 nM with Rexxip F to be used for the detection reagent. A 700 nM capture reagent was prepared with a 1:9 ratio of biotinylated TNF-α to biotinylated bovine serum albumin (b-BSA).

2.2.2 Comparing capture reagent concentrations

The binding capacity of the column can be adjusted by diluting the capture reagent with a biotinylated blocking protein that covers part of the binding sites on the column. This lowers the background by decreasing the amount of unspecific binding. It was suggested that I use biotinylated bovine serum albumin as a blocking protein.

I also compared two different types of Bioaffy CDs, the 1000 nl CD and the high-capacity 1000 nl CD. The high-capacity CD has different column beads that allows for more analyte to be captured. It could possibly increase the signal, but also the background by allowing for more unspecific binding.

Three different ratios of TNF-α to b-BSA was used as the capture reagent (1:19, 1:9 and 1:1), while all the other reagents was identical: 12.5 nM for the detection reagent and the same dilution series of TNF-α, which again was a 15 step series with concentrations from 164 nM to 0.025 pM. These conditions were used for both the 1000 CD and the 1000 high-capacity CD.

2.2.3 Determining the kinetic parameters of Humira and TNF-α

A dilution series of 12 samples of TNF-α was made from 100 nM to 3.9 pM. 1500 µl of 100 pM Humira was prepared in an Eppendorf tube. Both of these reagents were diluted in Rexxip A. 20 µl aliquots of the Humira were placed in the first four rows of a microtiter plate. Next a multichannel pipette was used to aspire 20 µl aliquots from the dilution series. These was added to the top row of the microtiter plate and mixed with the Humira by pipetting up and down a few times. A timer was started and one hour later TNF-α was added to the next row of the plate. The following additions were preformed 40 minutes later and then 30 minutes after that. Immediately after, the microtiter plate was loaded into a prepared Gyrolab Xpand. One last reaction series was prepared by mixing equal volumes of the dilution series and Humira and letting it incubate at room temperature for almost three days to let the reaction reach equilibrium fully.

2.3 Mixing CD 96

In microfluidic devices fluids move differently than what we are used to in our “macro-world”. Fluids flow laminarly. This allows for many of the unique applications that make microfluidics so useful, but in the rare cases when some turbulence is desirable one has to come up with some quite unique solutions. Mixing of two fluids is a common problem (Lee *et al.* 2011). Many microfluidic devices solve this problem by letting the fluids diffuse into each other, or adding structures that introduce some turbulence, but this requires long channels. Gyros have solved this in a novel way; by adding the two fluids and an air bubble in the same chamber in the CD. The Gyrolab then inverts the rotational speed of the CD 5 times every second. Making the air bubble shake, thus mixing the two fluids, as showed in figure 5.

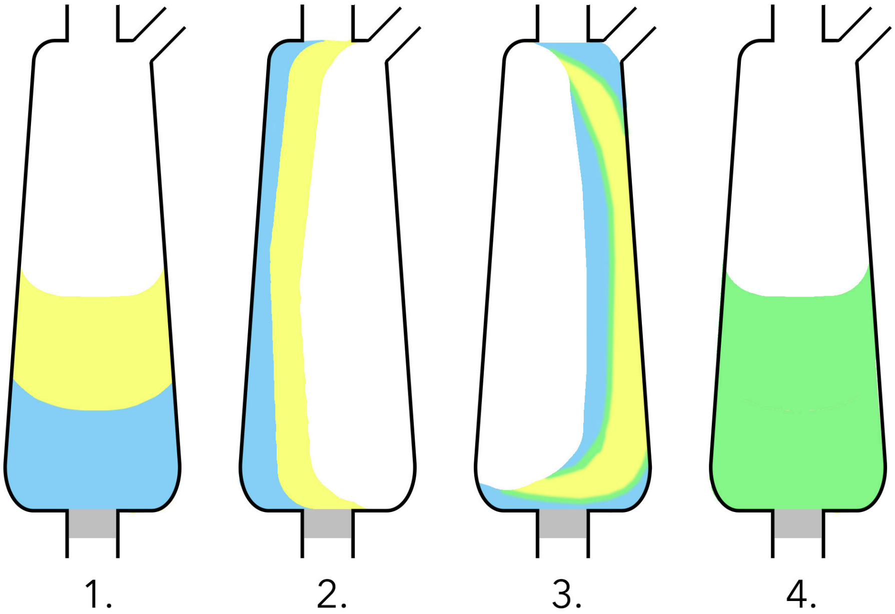

Figure 5: How the mixing chamber mixes two fluids. When the CD is at rest the bubble is located on top and the two fluids remain unmixed (1). When the CD starts to shake the bubble moves from side to side (2-3). The bubble moving in the chamber generates forces that shear the two fluids into each other and eventually the fluid is homogenous (4). Comparably to how the ingredients in bread dough can be mixed by kneading it. Figure created using Photoshop CC 2015.

Using the Mixing CD would reduce the manual work time and could make the results more reproducible since more steps would be preformed automatically.

The goal and main challenge in this sub-project was to create a *Gyrolab Method* that could be used to preform pre-equilibrium runs on the mixing CD. A Gyrolab method is basically a list of commands that the machine needs to execute a run. It defines how the needles that transfer the fluids in the machine are washed, how the spin sequences are ordered and much more. This proved more challenging than it might seem, since there are so many parameters that all influence the overall outcome. The key task of this method is that the dilution series needs to be mixed with the antibody at different time points. And since this had never been tried before on the mixing CD, there was no pre-set tools that I could use. I instead had to work around the problem, using other tools that would enable this seemingly simple task. The Gyrolab instrument has 8 mechanical syringes that it uses to transfer fluids from the microtiter plate to the CD. After the needles have been emptied on the CD they are moved to a wash station where they are washed with one or two wash solutions before aspiring from the next eight wells. What I hoped to accomplish was to delay some part of this process and make the transferred sample mix with a previously added solution on the CD. This delay would be the incubation time between two sample additions.

To achieve this I used a functionality called "Spin between transfer". This operation makes the CD spin while the needles are washed. It was possible to manually change the spin sequence to be much longer than the actual needle wash. Making the syringes wait for as long time as desired before they extruded the samples onto the CD. However, since the syringes withdraw the samples immediately after they have been washed, the samples stay in the syringes for the entirety of the incubation time. This could lead to unwanted effects, molecules in the samples could start to adsorb to the inside of the needle, or there could be some evaporation from the tip.

2.3.1 Reducing the background

Since the initial experiments on the mix CD had showed a very large background signal the capture reagent conditions were altered to reduce it. In the mixing CD the common reagents such as capture, detection and wash buffer are added in a larger volume than in the 1000 CD *(2.5 times as much is added).*

Therefore I first tried to lower the concentration of capture reagent from 700 nM to 280 nM so that an equal amount of biotinylated TNF-α would flow over the column. By recommendation from an employee of Gyros I also tried to change the ratio of TNF-α and BSA from 1:9 to 3:7.

5 nM of alexa tagged JDC-10 was used as detection reagent and a dilution series of Humira was made from 8192 pM to 0.5 pM in 15 steps.

2.3.2 Wash reagent test

After I presented my results to an employee at Gyros, she pointed out that it appeared that I had some carry-over in samples *(the first replicate was always higher than the second. This can be seen in figure 8)* After closer examination of the method's wash procedures, I saw that only the outsides of the needles were being washed. In all my previous experiments I had just used a mild wash buffer consisting of PBST. But it is recommended that a user use both this wash buffer and a more effective buffer that has some detergent properties. Therefore I created two new methods, identical with the previous method that generated fine curves *(except for the carry-over)* but one using both wash buffers and the other only the milder one, but washing the inside of the needles this time.

To compare the two methods a two time-point pre-equilibrium run was used. 150 pM of Humira was used. The dilution series was 8 steps and spanned from 32000 pM to 500 pM. 700 nM of Capture reagent was used which was a 3:7 ratio of b-TNF-α to b-BSA.

2.3.3 Incubation test

When the reaction takes place the CD should not be sitting still since this could lead to loss of fluids due to capillary forces acting in the corners of the channels. A phenomenon called "wicking" (Andersson *et al.* 2007), which is showed in figure 6 below. It was suggested that the CD should be mixed continuously and not just spun at a constant speed to best counter this. This came with a drawback though; each time the instruments changes speed, it needs a few lines of code, a shaking method would therefore be tens of thousands of lines long. This depleted the instrument's RAM, making the instrument crash or at least add long loading times. I instead chose to make a method that spun at a constant speed for a few seconds, then shook a short while, then spun again.

To investigate if it made a difference to spin or to shake the CD two methods were created that differed only in this regard. One spun at a constant speed for 20 minutes while the other spun for 5 seconds, shock for ~0.5 seconds and repeated.

The reagents were prepared in the same way as described in section 2.3.2.

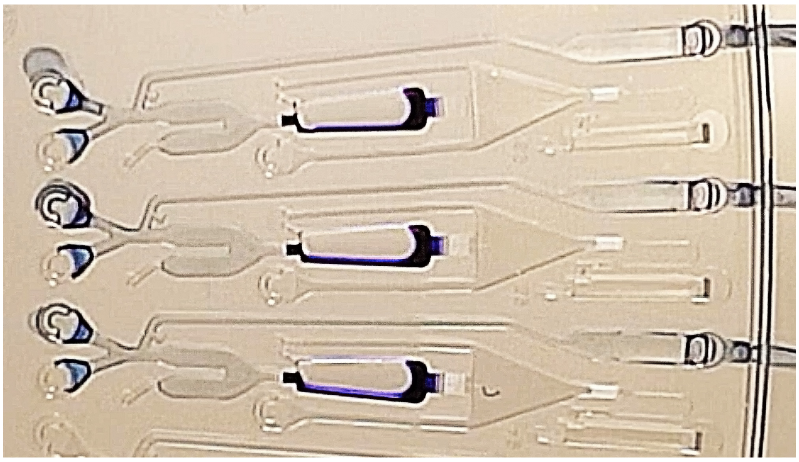

Figure 6: Three structures of the Mixing CD 96. Here with 100 nl coloured buffer in the mixing chamber. This CD has been lying still for a few minutes. Notice how the fluid has spread along the left side of the chamber wall. While the fluid is stopped by the hydrofobic barrier, this magnified surface area could drastically increase evaporation. That is why it is of great importance that the reaction mixture is forced to the bottom of the chamber. Photo taken with a Samsung galaxy S9+, 17th april. 2019. Uppsala, Sweden.

2.3.4 Comparing the Mix CD with the Bioaffy 1000

After having a method that gave adequate curves I compared it to the assay used for the 1000 CD.

A 16 step dilution series of TNF-α was made with concentrations from 500 nM to 6.18 pM. The capture reagent was 700 nM of a 3:7 ratio of b-TNF-α to b-BSA for both the CD-types. The detection reagent used was alexa tagged JDC-10, 12.5 nM for the Bioaffy 1000 and 5 nM for the Mix CD.

2.4 Anti-Avastin clones

Since the goal is to use my method to evaluate several drug candidates in parallel I needed to find a suitable model system. One that had several antibodies of varying kinetic and affinity but targeted to the same target protein. Thankfully such a system existed in-house at Gyros. It consisted of six so-called anti-idiotypic clones. An anti-idotype is an antibody that targets another antibody. A person's immune system eventually starts producing anti-idotypes after a treatment with antibody medicines. This small library of anti-idiotypes had previously been used to mimic the immune response to the drug Avastin. For all the experiments presented below biotinylated Avastin is the capture reagent and native Avastin is the varying interactant. The way the antibodies interact is illustrated below in figure 7. Since this system had been used before by Gyros there was data that suggested the appropriate span of the dilution series. The clones are all expressed in mouse cells, meaning that an anti-mouse detection antibody is used. This antibody is expressed in goat cells.

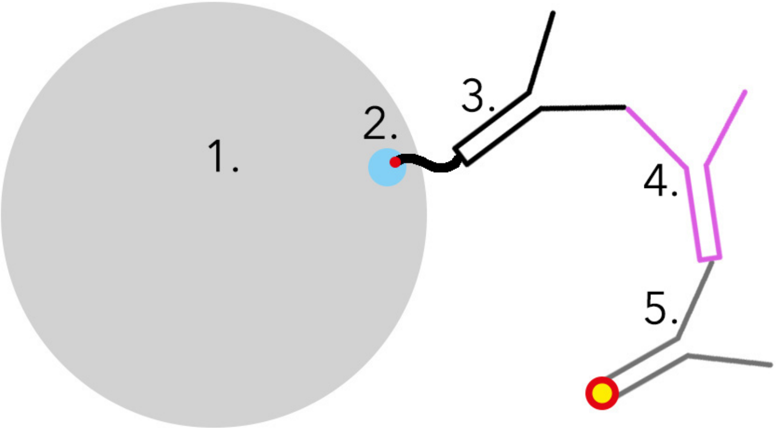

Figure 7: A schematic drawing of how the components are interacting in the column. The large grey bead (1) represents the column matrix, to which streptavidin is bound (2). The capture agent which here is biotinylated Avastin is bound through a linker (3). The clone (4), here in pink, binds to the Avastin and finally an anti-mouse antibody binds to the clone. This antibody has a fluorophore attached to it, which enables the detection (5).

2.4.1 Determining the limit of detection

The first step was to determine the limit of detection of all the clones so the fixed interactants concentration could be chosen. A 200 nl CD was used for this.

Dilution series of all clones were made; 8 steps with concentrations from 100 pM down to 0.0244 pM. 10 µg/ml of biotinylated Avastin was used as the capture reagent, and 10 nM of alexa-tagged anti-mouse antibody was used as the detection agent.

2.4.2 Individual runs

Each of the pre-equilibrium runs was preformed on the Bioaffy 200. Fresh dilutions were made for each experiment, and the fixed interactant and the variable interactant was mixed in a 1:1 ratio to start the reaction. All the reactions were started at the same time and then spun through the columns at different times. Three time points were generated with 20 minutes from the reaction start to the first and then 40 minutes between the first and second and second and third time point.

For clones 3, 4 and 5 an 11-step dilution series of Avastin was made with concentrations ranging from 25.6 nM to 5 pM. For clone 6 concentrations ranging from 15 μM to 586 pM of Avastin was used. For clone 23 and 28 concentrations from 15 μM to 14.3 pM. The concentrations for the clones were 120 pM for clone 3, 150 pM for clone 4 and 250 pM for clone 5. 5000 pM was used of clone 6, 2000 pM for clone 23 and 4000 pM for clone 28. 10 μg/ml of b-Avastin was used as capture reagent and 7.5 nM of the alexa tagged anti-mouse antibody was used as detection reagent.

2.4.3 Reproducibility test

To evaluate how robust the assay was and how reproducible the results are, I repeated the experiment for clone 5 four times. Using the same reaction conditions as described in section 2.4.2.

2.4.4 Determining the affinity with the conventional method

Two 12 step dilution series were made of Avastin. For clones 3, 4 and 5 concentrations from 51.2 nM down to 1 pM were prepared and for clones 6, 23 and 28 concentrations from 5.12 μM down to 100 pM were made. 1 nM of each clone as a fixed interactant. They were mixed in a 1:1 ratio in a microtiter plate and were left to incubate at room temperature for 24 hours covered with aluminium foil. For the capture reagent 10 μg/ml of b-Avastin was used and for the detection reagent 10 nM alexa tagged anti-mouse antibody was used.

3 Results

3.1 Initial experiments with the Bioaffy 1000

By implementing an equilibrium measurement the k_{off}-value of Humira could be accurately determined. When using a maximum incubation time of ~3 hours the k_{off}-value was much less accurate. The results compare well to reference data I found in an article by (Kaymakcalan *et al.* 2009), where the same interaction was studied using a Biacore Surface Plasmon Resonance (SPR). The results are found in table 1 below.

Table 1. Comparison between kinetic and affinity data generated from the novel method and from a SPR.

Parameter	Novel method	SPR (Biacore)
k_{on} ($M^{-1}S^{-1}$)	$8.72*10^5$	$1.69*10^6$
k_{off} (S^{-1})	$6.42*10^{-5}$	$4.71*10^{-5}$
K_D (M)	$7.37*10^{-11}$	$3.04*10^{-11}$

3.2 Mixing CD 96

The process of implementing the method on the Mix CD proved challenging, small improvements were continuously made, as exemplified in the comparisons in figure 8. Yet factors harder to control, such as evaporation had too large effect on the output.

3.2.1 Reducing the background

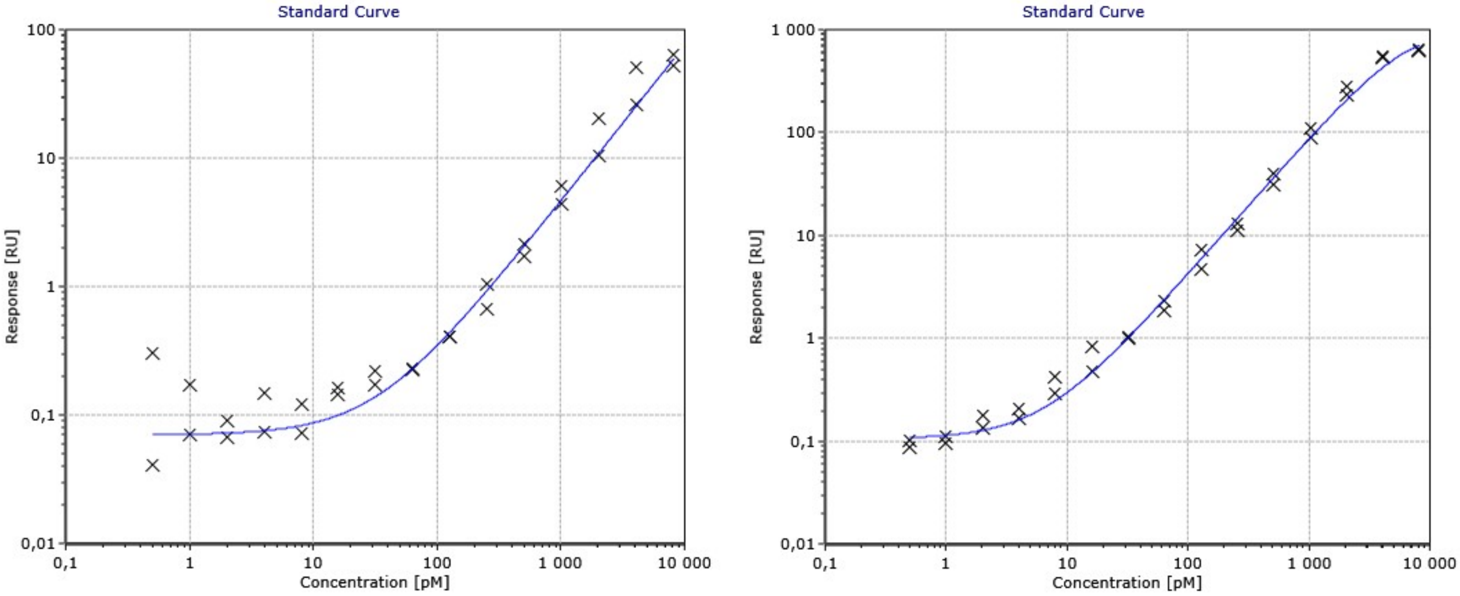

Figure 8: Comparison between using a 1:9 mixture of biotinylated TNFa and BSA versus a 3:7 mixture. Not only is the background signal lower when using the 3:7 mixture, but the variance between the replicates is lower as well.

3.2.2 Wash reagent test

There was no obvious difference in the comparison between using one wash buffer or two when rinsing the transfer needles. The problem with the carry-over disappeared once a proper wash procedure was implemented in the Gyrolab method. While this is true for this biological system, other proteins could more easily adsorb to the needles. I would therefore agree with Gyros recommendation to use both wash buffers when using a novel system.

3.2.3 Incubation test

If we look at the difference between the replicate pairs in figure 9, we see that there is not much difference when comparing the two incubation styles. The dispersion is however quite large, it would be a good idea to use more than two replicates if one wants to move forward with the mixing CD for kinetic screening.

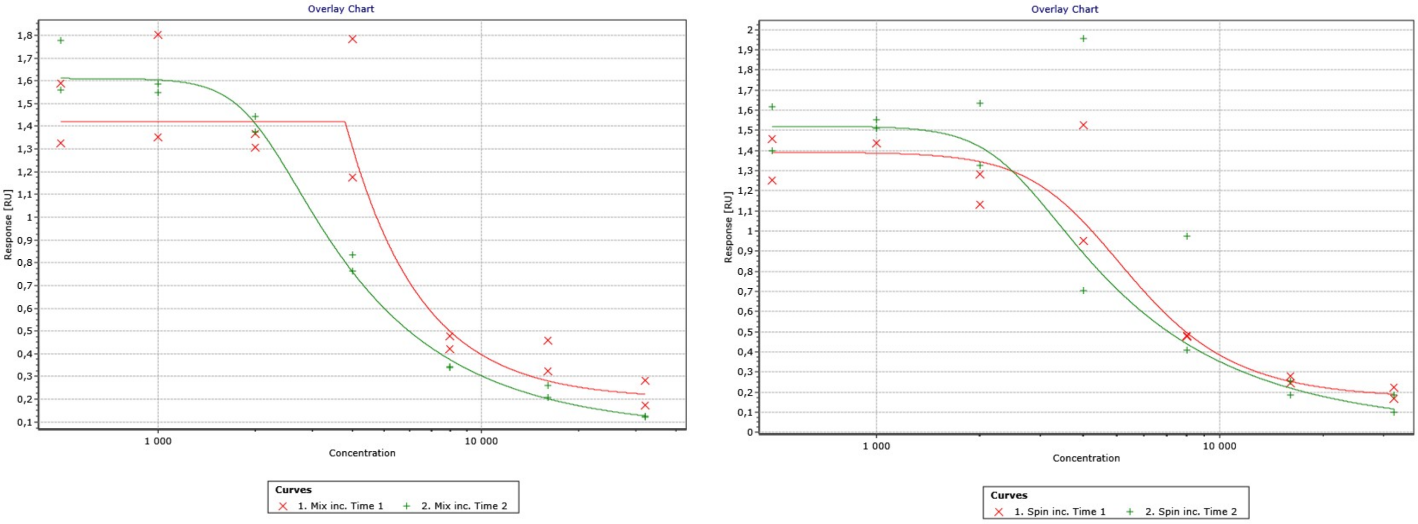

Figure 9: comparison between the two incubation styles; mixing to the left and spinning to the right. There is no drastic difference in the data quality. Neglect the curve fit here and only observe the dispersion of the data points.

3.2.4 Comparing the Mix CD 96 with the Bioaffy 1000

By looking at figure 10 it becomes obvious that there are some huge differences between the two CD types. The magnitude of the signal is not relevant here; rather observe the difference at where the titration starts to take place along the X-axis. This is troublesome since it means that the data generated from the mixing CD does not represent the bimolecular reaction in the same way as the Bioaffy 1000 does.

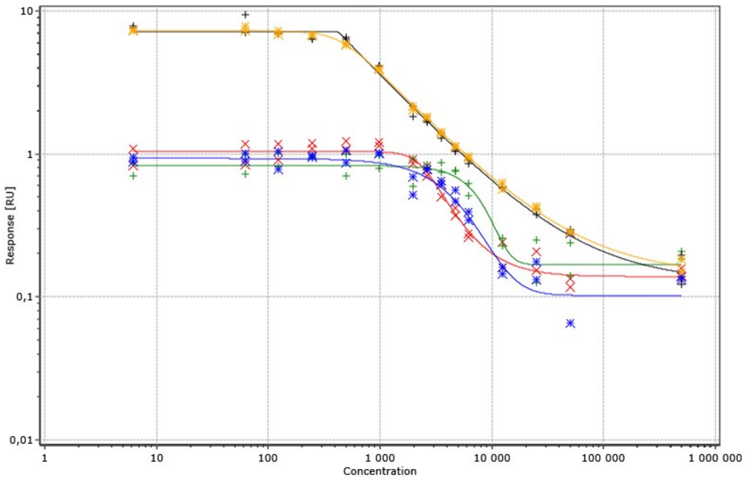

Figure 10: The same reaction performed on a mixing CD (yellow and black) and a Bioaffy 1000-CD(red, green and blue). Note how the titration of the mixing CD-reaction need an order of magnitude higher concentration of TNF-α before the signal start to decrease. The concentrations are in picomolar.

3.3 All clones

3.3.1 Determining the limit of detection

The limit of detection is used to choose the active concentrations of the clones for the individual runs. This is done by picking the concentration that generates a signal 10 times higher than the background.

3.3.2 Individual runs

Below in figure 11 is the data gathered from the anti-Avastin clones presented. Observe how the data points for clone 6 and 28 follow a different shape than for the remaining clones. I think this is an effect of the biology, which is further discussed in section 4.2.3.

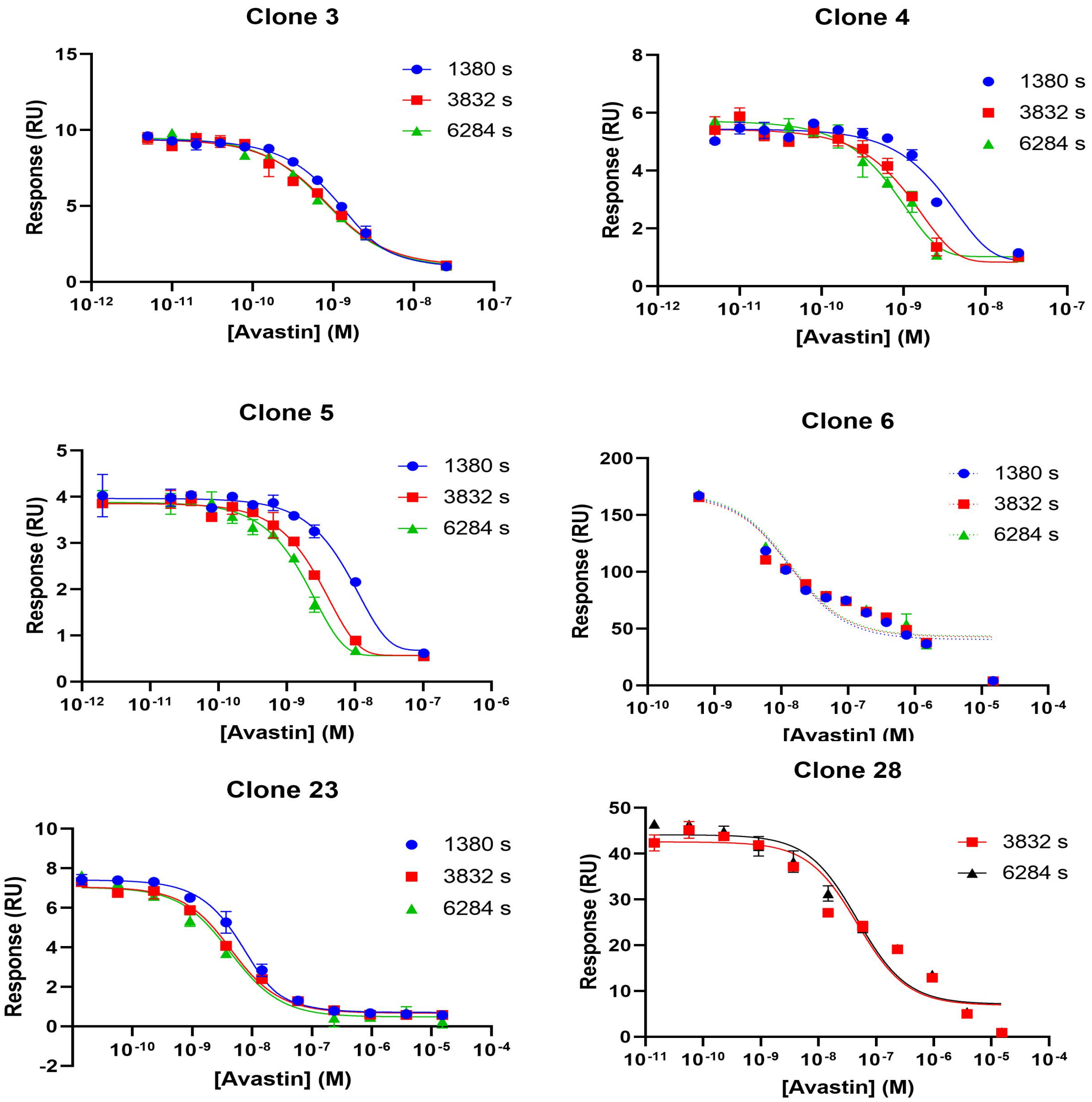

Figure 11: The inhibition curves of all six clones. Notice how the data distribution of clone 6 and 28 differs from the others, both in that they appear to reach equilibrium before the first analysis takes place *(since all curves are overlaid).* But by looking at the bulge at [Avastin] = 10^{-7} M it appears that the curves are made up by two curves. Figures created in GraphPad Prism 8.1.1.

The results in tables 1, 2, 4 and 5 have been calculated with a CI-value 95%. As seen in table 2 and 3, the unusual data distribution from clone 6 and 28 (Figure 11) impact the quality of the calculated values.

Table 2: The association rate constants of the clones calculated with the pre-equilibrium method.

Clone	k_{on} (Mean) ($M^{-1}s^{-1}$)	Lower limit ($M^{-1}s^{-1}$)	Upper limit ($M^{-1}s^{-1}$)
Clone 3	670000	522000	932000
Clone 4	168000	142000	225000
Clone 5	63000	57000	73000
Clone 6	~5340000000000	(Very wide)	(Very wide)
Clone 23	109800	81400	176000
Clone 28	~1090000	(Very wide)	(Very wide)

Table 3: The dissociation rate constants of the clones calculated with the pre-equilibrium method.

Clone	k_{off} (Mean) (s^{-1})	Lower limit (s^{-1})	Upper limit (s^{-1})
Clone 3	$4.471*10^{-4}$	$3.101*10^{-4}$	$6.811*10^{-4}$
Clone 4	$1.692*10^{-5}$	-inf	$1.196*10^{-4}$
Clone 5	$6.995*10^{-15}$	???	$4.767*10^{-5}$
Clone 6	66147	(Very wide)	(Very wide)
Clone 23	$4.548*10^{-4}$	$2.931*10^{-4}$	$8.175*10^{-4}$
Clone 28	~0.05023	(Very wide)	(Very wide)

Table 4: The dissociation constants of the six clones derived from the values of table 2 and 3, according to equation 3.

Clone	K_D (M)
Clone 3	$6.67*10^{-10} \pm 5.69 *10^{-11}$
Clone 4	$9.44*10^{-11} \pm 2.37 *10^{-10}$
Clone 5	$1.15*10^{-19} \pm 9.33 *10^{-11}$
Clone 6	$1.24*10^{-8}$ (Too large SD)
Clone 23	$4.14*10^{-9} \pm 3.99*10^{-10}$
Clone 28	$4.60*10^{-8} \pm$ (Too large SD)

Table 5: The dissociation constant calculated using Gyros conventional method ***(equation 3).***

Clone	K_D (Mean) (M)	Lower limit (M)	Upper limit (M)
Clone 3	$1.35*10^{-10}$	$9.10*10^{-11}$	$1.80*10^{-10}$
Clone 4	$7.74*10^{-11}$	$2.64*10^{-11}$	$1.28*10^{-10}$
Clone 5	$1.15*10^{-10}$	$8.00*10^{-11}$	$1.50*10^{-10}$
Clone 6	$1.53*10^{-8}$	$-1.94*10^{-11}$	$3.25*10^{-8}$
Clone 23	$2.33*10^{-9}$	$4.60*10^{-10}$	$4.20*10^{-9}$
Clone 28	$2.89*10^{-8}$	$-2.20*10^{-9}$	$6.01*10^{-8}$

3.3.3 Reproducibility test

The data from the reproducibility test are summarized in figure 12 below. The k_{off}-values could not be accurately determined for this clone. Note that the last replicate is somewhat lower than the others. This is most likely because of an unforeseen delay in the experiment which resulted in that the time to the first data-point is much less accurate the for the others, still the calculated values are not to far off from the other three replicates.

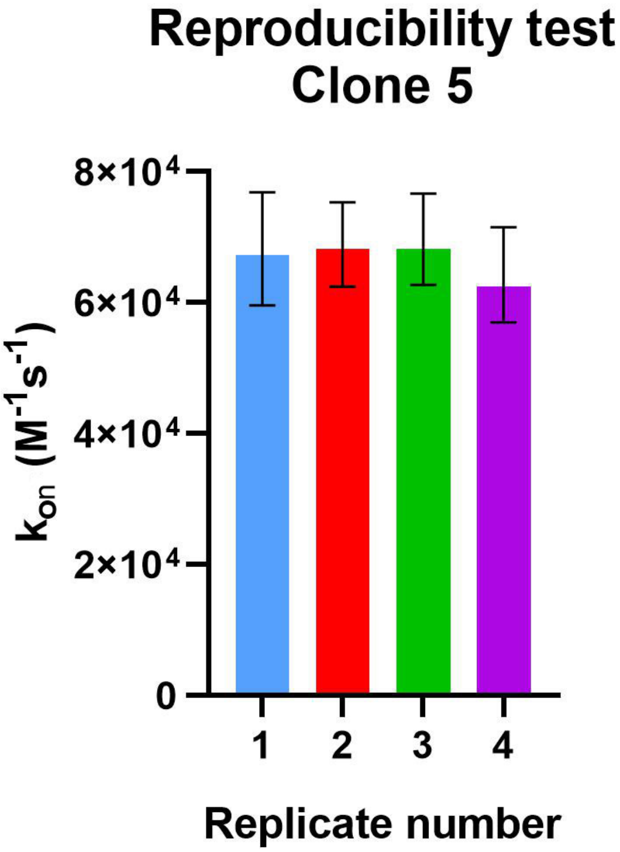

Figure 12: The data from the reproducibility test summarized in a bar plot. Figure created in GraphPad Prism 8.1.1

4 Discussion

Since the main goal of this master thesis was to develop an experimental method for pre-equilibrium measurements I here outline the method that I found to be most robust and simple to use.

4.1 Experimental method for pre-equilibrium kinetic characterization using Gyrolab

Find the limit of detection (LOD) for your analyte by diluting what will be the fixed interactant. Start with a high nanomolar concentration and dilute by a factor of 4 until low picomolar concentration. Select a concentration that gives a signal that is at least 10 times above the background to assure a linear correlation between the signal and the actual concentration of analyte in the entire titration. It is best not to select a too high concentration because this both makes the reaction reach equilibrium faster, but also makes determining the kinetic parameters harder since the terms in which they appear in the model will be dominated by the concentrations, see equation 10.

If no previous information about the fixed interactants affinity exists, preform a wide-range affinity measurement to know when the titration occurs. Do this by using a span on the varying interactants concentrations with ten-fold dilution. Observe where the titration takes place and for the next experiment use a two-fold dilution in that exact concentration area.

By queuing multiple copies of the same Gyrolab run and mixing the variable interactant with the fixed as described in section 3.1 we get the desired time-series.

Export the data to suitable software to preform non-linear curve fitting with the pre-equilibrium model.

4.2 Limitations and how to circumnavigate them

4.2.1 Reactions with slow dissociation

As seen in table 1 and 2, this new method appear to be more suited to calculate k_{on} rather than k_{off} for this library of anti-idiotypic clones. It would appear that when k_{off} drops to $\sim10^{-5}$ s^{-1} the dissociation has too small effect on the reaction to be measured directly. But as showed in the introduction k_{off} can be calculated by multiplying K_D with k_{on}, as per equation 3. This approach; to measure k_{on} and K_D separately is a solution used by an other company called Sapidyne in their KinExA product line (Bee *et al.* 2012). Luckily the K_D can easily be determined with Gyros existing software using the equilibrium approach. Using these methods in combination, it is possible to still preform a full kinetic characterization of the antibodies. Using this method I could easily determine the k_{off} values of clone 4 and 5, the results are presented in table 7 below. However, an even simpler approach is what was done in the Humira experiment, where longer incubation times were used. Here I waited until equilibrium for the last measurement, however I think this is not necessary, one should rather have a time point much later that "anchors" the data. Another benefit of doing it this way instead of waiting all the way until equilibrium is that it is not obvious when a reaction has reached equilibrium. Will it happen after three hours? One day? Three days? The simplest way of knowing this is to preform multiple runs and see when the curves have stopped moving. This is however not necessary when using the pre-equilibrium approach.

Table 6: The calculated k_{off}-values using data from both the pre-equilibrium approach and from the conventional method.

Clone	k_{off}
Clone 4	$1.30*10^{-5}$ s^{-1}
Clone 5	$7.29*10^{-6}$ s^{-1}

But using this approach means that one is missing out on one of the great advantages of the pre-equilibrium method. One in fact has to wait until equilibrium. It should be pointed out that it is very possible to simply increase the time between the measurements, which might give the reaction more time to be influenced by the dissociation. When characterizing the clones, 40 minutes passed between every reaction series that was analysed. By adding long pauses in the Gyrolab methods, this time can be increased indefinitely. Alternatively, if one does not wish to occupy the instrument for an exorbitant amount of time the "Analyse simultaneously"-method described in 3.1 can be used. Indeed, when using this approach to characterize Humira both k_{on} and k_{off} could be determined accurately.

4.2.2 Fast reactions

If the reaction reaches equilibrium so fast so that no clear difference can be seen in-between the time points, such as clone 6, it is not possible to calculate the kinetic parameters. Generally speaking though, antibody systems that reach equilibrium fast are often low affinity ones (Pollard 2010), and therefore less interesting in drug development.

Clone 23 reached equilibrium fast as well, so to lower the incubation time I tried implementing it on the mix CD using a 5-minute incubation time. And while the curves were more separated, they could not provide good data. Actually the run preformed on the 200 bioaffy provided pretty good data (Figure 11). This indicates that as long as there is some separation between the curves the kinetic parameters can be calculated with relative precision. However this direct comparison also indicates that the Mixing CD is not adequate for these types of experiments. But this will be further examined in section 4.2.4

4.2.3 Biology is complex

The biological systems that I have examined in this project are not as simple as the model would have you think. To describe an antibody binding its antigen as $A + B \Leftrightarrow C$ is a big simplification. However it is the standard way of doing it because the results one obtain is good enough (Björquist & Boström 1997). Yet researchers often come up with their own, more complex models (Kaufman & Jain 1992, Müller *et al.* 1998, van Steeg *et al.* 2016). An antibody has two points where it can bind the antigen, so a model such as the one presented below might be more accurate.

$$\mathrm{A} + 2\mathrm{B} \;\Leftrightarrow \mathrm{AB} + \mathrm{B} \;\Leftrightarrow \mathrm{AB}_2$$

As mentioned, the simpler model generates results that are good enough, but I have seen some abnormalities in my data that could be explained by this simplification. Mainly the small bulge in the data just before the curve starts to decrease. This phenomenon can be observed in almost every dataset that I have generated *(can be seen quite clear in figure 10, and note that the y-axis is logarithmical)* and seem to indicate that the antibody has higher affinity for the capture agent when there is a tiny amount of antigen present. This could be because that the antibody has been "primed" as in it has higher affinity towards the antigen once it has captured and released an antigen. This would however mean that this phenomenon would be less prevalent in the antibodies with slower off-rate such as clone 5. But this does not seem to be the case. I think a more reasonable explanation is that an antibody that has bound one antigen now has a slightly higher affinity for the next antigen. At low concentrations the majority of antibodies that binds to a target only binds to one, meaning that the overall affinity to the capture agent is increased. Which can be observed as a slight increase in the signal before antibodies start to bind to antigens and the concentration of antigen in solution is decreased.

The unusual shape of the data of clones 6 and 28 can also be blamed on the fact that their interaction with Avastin does not follow the simple A + B ⇔ C model. There is also the possibility that the antibodies can form multi-unit complexes when both interactants are antibodies. To accurately model this system one would need to preform other studies to figure out how the antibody binds to its antigen.

4.2.4 The Bioaffy 96 Mix

In direct comparisons between the mixing CD and the 1000 Bioaffy, we can see that the curves have different characteristics. Namely that the titration begins later when using the mixing CD *(figure 10).* This could be because of evaporation because we can observe this phenomenon when comparing longer incubation times *(30 minutes)* but this is absent when the incubation time was only 5 minutes *(Data not showed).* This CD is not made for these types of experiments, so it should come as no surprise that it proved difficult to implement the assay on it. There are many factors that impact the output. Maybe by optimising all of these in a more systemized fashion than I did could lead to a functional method.

Some small software changes could also lead to big improvements. It was mentioned before that the needles aspire more sample immediately after they have been washed. If the incubation step is much longer than the needle wash the sample will remain in the needles for a long time, which could have adverse effects. If the instrument was programmed to delay the sample aspiration for as long as possible this potential problem could be solved immediately. Some changes to the user interface when designing new methods would also be beneficial before releasing this potential product. Namely those that would make selecting the incubation time more simple.

4.3 Column profile analysis

Lets preform a thought experiment: First, lets envision an irreversible chemical reaction, of the type $A + B \xrightarrow{k_{on}} C$. Where A is an antibody in solution and B is a capture reagent immobilized on a column. If we consider this a stochastic process then the distribution of A along the column should be shaped as a normal distribution where the width is dependant of k_{on}, the higher k_{on} the narrower the distribution is and vice versa.

If we next consider a reaction such as:

$$\mathrm{A} + \mathrm{B} \underset{\mathrm{k_{off}}}{\overset{\mathrm{k_{on}}}{\rightleftarrows}} \mathrm{C}.$$

We would receive a different type distribution along the column. It would still be a normal distribution dependant only on k_{on}, but it would have a “tail-section" that is dependant of the k_{off} and k_{on}. If we look at some well-defined column profiles, this is exactly what we see! (Figure 13) There has been some research into this already, for example, in an elution profile of an affinity chromatography column, the natural logarithm of the slope of the tail is the k_{off}. But this in only applicable if the analyte cannot re-bind to the column. It is most likely possible to deduce mathematical formulas that can accurately calculate both k_{on} and k_{off}. But a simpler solution is to rank peak widths and tail lengths of known antibodies, and then use this as a regression tool when selecting starting guesses when one analyses completely novel antibodies.

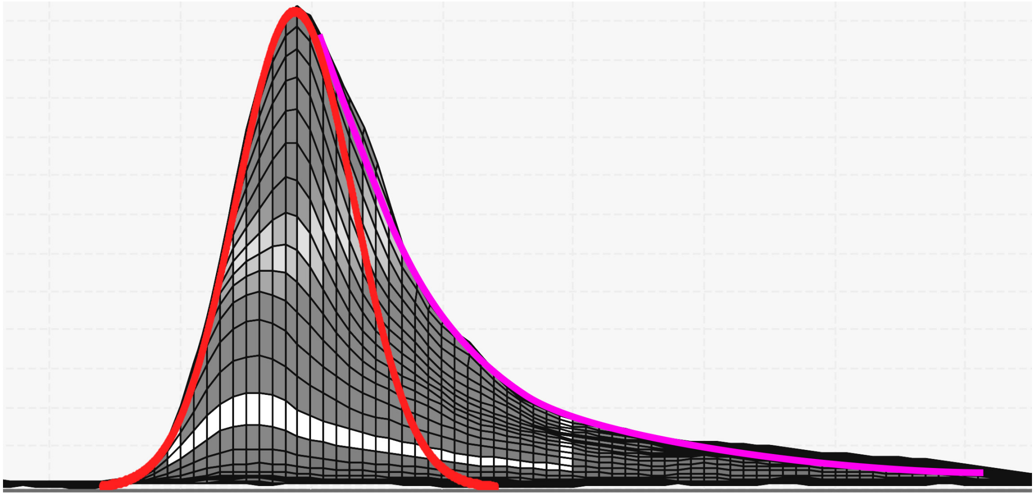

Figure 13: A column profile with a normal distribution overlaid the main body of the profile (red) and an exponential overlaid the tail section (pink)

4.4 Conclusions

This novel method has proven to accurately and robustly determine kinetic parameters. Just as with existing methods the dissociation rate constant is sometimes hard to determine though, this can be circumnavigated by calculating it from the association rate constant and the dissociation equilibrium constant. This demands an equilibrium measurement to be made, which loses one of the biggest advantages of the pre-equilibrium method. But since this method still is both label free and in solution, as well as demands small sample volumes, the benefits of this novel method are clear. The next step for this method should be to evaluate more drug candidates, preferably from a real world pharmaceutical project. If successful, this would strengthen the claim that the method does have its place on the scientific market. It would also be beneficial to perform further comparisons with other methods, namely SPR and KinExA. Not only to compare the calculated values, but also time, cost and ease of use. Since the Gyrolab is a well-established technology, it should hopefully be superior in at least one of these regards!

5 Acknowledgements

First I would like to express my gratitude to my supervisor Johan Engström for always showing enthusiasm and curiosity during this project and for sharing his encyclopaedic knowledge about the field of Life Science. I must also thank everyone at Gyros who have answered my myriads of questions.

I would like to acknowledge my subject reader Professor Magnus Johansson for sharing his theoretical expertise and for introducing, and making me interested in biophysics in the first place.

I would also like to thank my student opponent Oscar Boström for his thoughtful and precise feedback.

Thank you.

6 Bibliography

Alberts B, Johnson A, Lewis J, Morgan D, Raff M. 2014. Molecular Biology of the Cell. Taylor and Francis, Oxford, UNITED KINGDOM.

Andersson P, Jesson G, Kylberg G, Ekstrand G, Thorsén G. 2007. Parallel Nanoliter Microfluidic Analysis System. Analytical Chemistry 79: 4022–4030.

Bee C, Abdiche YN, Stone DM, Collier S, Lindquist KC, Pinkerton AC, Pons J, Rajpal A. 2012. Exploring the Dynamic Range of the Kinetic Exclusion Assay in Characterizing Antigen-Antibody Interactions. PLOS ONE 7: e36261.

Björquist P, Boström S. 1997. DETERMINATION OF THE KINETIC CONSTANTS OF TISSUE FACTOR/FACTOR VII/FACTOR VIIA AND ANTITHROMBIN/HEPARIN USING SURFACE PLASMON RESONANCE. Thrombosis Research 85: 225–236.

Burness CB, Deeks ED. 2012. Adalimumab. Drugs 72: 2385–2395.

Chames P, Van Regenmortel M, Weiss E, Baty D. 2009. Therapeutic antibodies: successes, limitations and hopes for the future. British Journal of Pharmacology 157: 220–233.

Eckersten A, Örlefors AE, Ellström C, Erickson K, Löfman E, Eriksson A, Eriksson S, Jorsback A, Tooke N, Derand H, Ekstrand G, Engström J, Honerud A-K, Aksberg A, Hedsten H, Rosengren L, Stjernström M, Hultman T, Andersson P. 2000. High-Throughput SNP Scoring in a Disposable Microfabricated CD Device. In: van den Berg A, Olthuis W, Bergveld P (ed.). Micro Total Analysis Systems 2000, pp. 521–524. Springer Netherlands,

Giuliani M, Bartolini E, Galli B, Santini L, Surdo PL, Buricchi F, Bruttini M, Benucci B, Pacchiani N, Alleri L, Donnarumma D, Pansegrau W, Peschiera I, Ferlenghi I, Cozzi R, Norais N, Giuliani MM, Maione D, Pizza M, Rappuoli R, Finco O, Masignani V. 2018. Human protective response induced by meningococcus B vaccine is mediated by the synergy of multiple bactericidal epitopes. Scientific Reports 8: 1–15.

Gustafsson M, Hirschberg D, Palmberg C, Jörnvall H, Bergman T. 2004. Integrated Sample Preparation and MALDI Mass Spectrometry on a Microfluidic Compact Disk. Analytical Chemistry 76: 345–350.

Honda N, Lindberg U, Andersson P, Hoffmann S, Takei H. 2005. Simultaneous Multiple Immunoassays in a Compact Disc–Shaped Microfluidic Device Based on Centrifugal Force. Clinical Chemistry 51: 1955–1961.

Hulme EC, Trevethick MA. 2010. Ligand binding assays at equilibrium: validation and interpretation. British Journal of Pharmacology 161: 1219–1237.

Kaufman EN, Jain RK. 1992. Effect of bivalent interaction upon apparent antibody affinity: experimental confirmation of theory using fluorescence photobleaching and implications for antibody binding assays. Cancer Research 52: 4157–4167.

Kaymakcalan Z, Sakorafas P, Bose S, Scesney S, Xiong L, Hanzatian DK, Salfeld J, Sasso EH. 2009. Comparisons of affinities, avidities, and complement activation of adalimumab, infliximab, and etanercept in binding to soluble and membrane tumor necrosis factor. Clinical Immunology (Orlando, Fla) 131: 308–316.

Kazazi-Hyseni F, Beijnen JH, Schellens JHM. 2010. Bevacizumab. The Oncologist 15: 819–825.

Lee C-Y, Chang C-L, Wang Y-N, Fu L-M. 2011. Microfluidic Mixing: A Review. International Journal of Molecular Sciences 12: 3263–3287.

Müller KM, Arndt KM, Plückthun A. 1998. Model and Simulation of Multivalent Binding to Fixed Ligands. Analytical Biochemistry 261: 149–158.

Pollard TD. 2010. A Guide to Simple and Informative Binding Assays. Molecular Biology of the Cell 21: 4061–4067.

Salimi-Moosavi H, Rathanaswami P, Rajendran S, Toupikov M, Hill J. 2012. Rapid affinity measurement of protein–protein interactions in a microfluidic platform. Analytical Biochemistry 426: 134–141.

Urquhart L. 2019. Top drugs and companies by sales in 2018. Nature Reviews Drug Discovery 18: 245.

van Steeg TJ, Bergmann KR, Dimasi N, Sachsenmeier KF, Agoram B. 2016. The application of mathematical modelling to the design of bispecific monoclonal antibodies. mAbs 8: 585–592.

Vanhove E, Vanhove M. 2018. Affinity determination of biomolecules: a kinetic model for the analysis of pre-equilibrium titration curves. European biophysics journal: EBJ 47: 961–966.